Probing Bioluminescence Resonance Energy Transfer in Quantum Rod – Luciferase Nanoconjugates

*Rabeka Alam,[1]♮ Liliana M. Karam,[1] Tennyson L. Doane,[1] Kaitlin Coopersmith,[1] Danielle M. Fontaine,[3] Bruce R. Branchini,[3] Mathew M. Maye[1,2]**

[1]Department of Chemistry Syracuse University, Syracuse New York, 13244
[2]Syracuse Biomaterials Institute, Syracuse University, Syracuse New York, 13244
[3]Department of Chemistry, Connecticut College, New London Connecticut, 06320
♮*Present Address*: Radiation Laboratory, Department of Chemistry & Biochemistry, University of Notre Dame, Indiana, 46556
******mmmaye@syr.edu*

Materials. Cadmium oxide (CdO, 99.99%), trioctylphosphine (TOP, 90%), trioctylphosphine oxide (TOPO, 90%), octadecene (ODE, 90%), methylphosphonic acid (MPA, 98%), sulfur (S, 100 mesh), zinc acetate ($ZnAc_2$, 99.99%), octylamine (OAm, 99%), didecyldimethylammonium bromide (DDAB, 98%), Gold (III) chloride hydrate ($HAuCl_4$, 99.99%), dodecylamine (DDA, 99%) olelyamine (OAm, 90%), L-histidine (His, >99.8%), sodium borohydrate ($NaBH_4$, >96%), sodium tetraborate (99.5%), boric acid (>99.5%), toluene (≥99.5%), chloroform (>99.8%), methanol (>99.8%), acetone (99.5%), and (11-mercaptoundecyl)tetra(ethylene glycol) (PEG, 90%) were purchased from Sigma Aldrich. Selenium (Se, 200 mesh 99.99%) was purchased from Alfa Aesar. Octadecylphosphonic acid (ODPA, 98%) and hexylphosphonic acid (HPA, 98%) were purchased from Strem Chemicals. Ultrapure water (18.2 MΩ) was provided from a Sartorius Stedim Arium 61316 reverse osmosis unit combined with an Arium 611DI polishing unit. The adenosine 5'-triphosphate magnesium salt (Mg-ATP, > 95%) was purchased from Sigma-Aldrich, and restriction endonucleases from New England Biolabs (Beverly, MA). D-Firefly luciferin (LH_2) and benzothiophene luciferin ($BtLH_2$) were generous gifts from Promega (Madison, WI).

Synthesis

Core Shell Quantum Rods (QR) with rod-in-rod (r/r) morphology: The CdSe/CdS *r/r*-QRs with emission at 615 nm (QR(615)), were synthesized with CdSe rod shaped cores by modifying a literature technique.[1,2] First, CdO (0.47 mmol), TOPO (7.7 mmol), DPA (0.90 mmol), and 2 mL of ODE were combined in a four-neck round-bottom flask that was heated to 150 °C under vacuum for one hour. The CdO was dissolved by heating to 340 °C in Ar gas where the reaction mixture changed color from red-brown to clear and colorless. Then 0.5 mL of TBP was added, followed by Se (0.63 mmol) dissolved 1 mL of TBP previously prepared in a glove box. The TBP=Se was swiftly injected into the reaction mixture, and the growing QRs were annealed for 10 minutes, and then let to cool. An aliquot (1~3 mL) of toluene was added at 60 °C to limit solidification, and then the QR was precipitated using methanol and dispersed in toluene (Figure S1). Next, a CdS rod shell was grown by preparing a mixture of CdO (0.23 mmol), TOPO (7.7 mmol), ODPA (0.42 mmol), HPA (0.24 mmol) and 2 mL of ODE, that was heated to 150 °C under vacuum for 1 h, then heated to 340 °C similarly to above. The temperature was then increased to 365 °C and CdSe cores (160, 320, or 640 nmol) and sulfur (0.06 g, 1.9 mmol) were

dissolved together in 2.0 mL of TOP, which was quickly injected and annealed for 10 min, let cool to room temperature, and then the CdSe/CdS were purified as described above. The QR with *s*-, *m*-, and *l*-aspect ratios were grown by tailoring the amount of cores used. The QR(650) were prepared using new ODPA (0.75 mmol) and MPA (0.08 mmol) amounts, while other conditions were the same. The CdSe shells of QR(650)-*s*, -*m*, and –*l*, were prepared identically to that for QR(615), by systematic change to core concentration (5, 10, or 20 nmol) during injection. See SI for more details and for chemical abbreviations.

AuNP growth on QR: For gold nanoparticle (AuNP) growth on QRs,[3] a reaction solution was made by dissolving $HAuCl_4$ (2.5 mg), DDA (35.0 mg), DDAB (20.0 mg) in 4 mL of toluene and sonicating the solution. This was then added to the QR (0.10 nmol) in 10 mL of toluene. The mixture was stirred under Ar in room temperature and room light for 24 h. AuNP growth was indicated by the quenching of fluorescence and change in solution color.

Ppy Expression: The plasmids for hexahistine tagged PpyGRTS and PpyRE9 were constructed by excising the corresponding genes for PpyGRTS and PpyRE9 from the pGEX-6P-2 vector and ligating them into a modified pQE30 expression vector using previously described procedures.[4–6] The His-tagged proteins were expressed and purified as earlier reported.[6] The proteins were stored at 4 °C after they were dialyzed against 50 mM Tris_HCl (pH 7.0) containing 150 mM NaCl, 1.0 mM EDTA, 1.0 mM DTT, 0.8 M ammonium sulfate and 2%.

Histidine-Mediated Phase transfer & Ppy Conjugation: The QR were phase transferred to aqueous buffers using our Histidine-mediate phase transfer protocol.[7,8] The organic ligands of the QR were directly exchanged with *L*-histidine (His), rendering them hydrophilic. This was achieved by adding a [His]:[QR]~5000-fold molar excess.[9] The His-solution was prepared by dissolving in a basic 3:1 $MeOH/H_2O$ solution. Then and aliquot was added to purified QRs dispersed in chloroform and vortexed for 1 minute. This resulted in the QRs being transferred to the aqueous layer, to 10 mM borate buffer (pH 8.3). Excess organic ligands were back-extracted by addition of fresh chloroform, vortexing, and decanting of the organic solution. This extraction procedure was repeated at least four times. Then excess His was removed by rinsing the hydrophilic QRs with 10 mM borate buffer using a 100kDa molecular weight centrifugal filter (Millipore). Finally the QRs were dispersed in 10 mM borate buffer and refrigerated before use. The QR using estimates based on QR volume, see SI. Next, the Ppy were incubated with His-QRs at increasing molar ratios, L = [Ppy]:[QR] from 1-40. The conjugates were let to react for at least 15 min before measurements. Typical [QR] during incubation as ≈ 500 nM.

Measurements: The BRET experiments were carried out in a similar manner to previous reports.[2,10,11] In a typical BRET experiment, a mixture of 100 μL of 91 μM LH_2 (D-firefly luciferin) and 30 μL of 8.66 mM Mg-ATP in 25 mM gly-gly buffer (pH 7.8) was added to the Ppy-QR conjugate solution in a 96-well plate and bioluminescence emission is immediately collected using a Varian Cary-Eclipse spectrophotometer in bioluminescence /chemiluminescence mode. White 96-well plates were employed, with volumes ranging from 50-200 μL. Bioluminescence spectra were collected every 15 seconds for 7.5 minutes. The presented BRET results are the average of the first five spectra collected over 1.5 min after addition of LH_2. The instrument was corrected for detector sensitivity by comparison of fluorescence standard emission intensities (500 – 800 nm) with a corrected detector on a Fluoromax-4 spectrophotometer. Final peak area was calculated by spectral deconvolution of each spectrum, and BRET ratios (*BR*) was

determined by taking a ratio of QR and Ppy emission intensities. For more information on calculations and measurements see SI.

Calculations

QR Concentration: The concentration of QR was calculated based on UV-vis optical absorption at 350 nm using extinction coefficients (ε_{QR}) based on the average volume of the QRs.[12] The final concentrations were obtained using the Beer-Lambert equation, Abs = εbc; where ε is the estimated extinction coefficient (M^{-1} cm^{-1}), b is the path length, and c is concentration. A tabulation of the calculated ε values is given in Table S1.

QR Quantum Yield (QY): The QR photoluminescence quantum yields (QY) were calculated based on comparison to a reference dye using standard methods (equation 1):[13]

$$QY_{qdot}(\%) = QY_R\left(\frac{Abs_R}{Abs_{qdot}}\right)\left(\frac{PL_{qdot}}{PL_R}\right)\left(\frac{\eta^2{}_{qdot}}{\eta^2{}_R}\right) \qquad (1)$$

where QY_R is the reference dye quantum yield (Rhodamine 6G = 95%), Abs_R and Abs_{QD} are the optical absorption at specific excitation for the reference dye and QR samples respectively. PL_R and PL_{QD} correspond to the total area of the PL emission after wavelength dependent calibration of both the excitation source, and photoluminescence detector, as well as after PL spectra baseline correction.

Förster Resonance Energy Transfer (FRET) & Optical Anisotropy: In this study, the bioluminescence resonance energy transfer (BRET) constants were calculated in the identical manner to FRET. In FRET, the Förster distance (R_0) is calculated using equation 2:[13,14]

$$R_0 = 9.78 \times 10^3((\kappa^2 n^{-4} Q_D J(\lambda))^{1/6} \qquad (2)$$

where n refractive index of the medium (n = 1.33), κ is the dipole orientation factor (κ = 2/3), Q_D is the donor quantum yield QY(GRTS) ≈ 32%, and $J(\lambda)$ is the spectral overlap integral. The $J(\lambda)$ value can be calculated using equation 3:

$$J(\lambda) = \int F_D(\lambda)\varepsilon_A(\lambda)\lambda^4 d\lambda \qquad (3)$$

where λ is the defined wavelength of the donor-acceptor spectral overlap, and $F_D(\lambda)$ is the integrated donor emission with area normalized to unity, and $\varepsilon_A(\lambda)$ represents the acceptor extinction coefficient at the particular wavelength. When $\varepsilon_A(\lambda)$ is in units of $M^{-1}cm^{-1}$, and λ is in units of cm, the units for $J(\lambda)$ are M^{-1} cm^3.

Using the R_0 values calculated above, the FRET efficiency, E, was calculated using equation 4:[13,14]

$$E = 1 - \frac{F_{DA}}{F_D} = \frac{R_0{}^6}{R_0{}^6 + r^6} \qquad (4)$$

where F_{DA} is donor fluorescence in the presence of acceptor, and F_D is fluorescence of the donor without acceptor. A tabulation of the calculated BRET constants is shown in Table S1 and S3.

Fluorescence anisotropy (<*r*>) measurements were collected using an L-shape spectrometer set-up and a Fluoromax-4 spectrofluorometer equipped with automatic emission and excitation polarizers. The <r> was calculated by :[13]

$$< r >= \frac{I_{\parallel} - I_{\perp}}{I_{\parallel} + 2I_{\perp}} \qquad (5)$$

where $I_{\parallel}$ and $I_{\perp}$ are the fluorescence intensities polarized parallel and perpendicular to the excitation polarization, respectively. The anisotropy values vary from -0.2 (where the absorption and fluorescence dipole moments are perpendicular) to 0.4 (where they are perpendicular). Excitation anisotropy measurements of each QR was performed using 1nm slit widths.

The orientation factors (κ) values were calculated using:

$$\kappa = \hat{\mu}_D \cdot \hat{\mu}_A - 3(\hat{\mu}_D \cdot \hat{R}_{DA})(\hat{\mu}_A \cdot \hat{R}_{DA}) \qquad (6)$$

where $\hat{\mu}_D$ is the vector along the transition dipole of the donor, $\hat{\mu}_A$ is the vector along the transition dipole of the acceptor, and $\hat{R}_{DA}$ is the vector between the two transition dipole moments. For anisotropic systems, the κ^2 can theoretically vary from 0 (where the transition dipole moments are perpendicular in plane) to 4 (where the transition dipole moments are parallel in plane, for example).

The QR PL-decay determined lifetimes were determined by fit to a bi-exponential decay function after correction for instrumental response function:

$$I(t) = I_0 + a_1 \exp\left\{\frac{-(t - t_0)}{\tau_1}\right\} + a_2 \exp\left\{\frac{-(t - t_0)}{\tau_2}\right\} \qquad (7)$$

were *I* is the intensity in counts, t_0 is the off-set time determined by the instrumental response, and τ_1 and τ_2 are the determined lifetimes.

Measurements

The BRET experiments were carried out as described recently.[2,10,11] In a typical BRET experiment, a mixture of 100 μL of 91 μM LH_2 (D-firefly luciferin) and 30 μL of 8.66 mM Mg-ATP in 25 mM gly-gly buffer (pH 7.8) is quickly added to the Ppy-QR conjugate solution in a 96-well plate and bioluminescence emission is immediately collected. The bioluminescence and BRET were collected on a Varian Cary-Eclipse spectrophotometer in bioluminescence /chemiluminescence mode using a 96-well plate reading accessory. White 96-well plates were employed, with volumes ranging from 50-200 μL. Bioluminescence spectra were collected every 15 seconds for 7.5 minutes. The instrument was corrected for detector sensitivity by comparison of fluorescence standard emission intensities (500 – 800 nm) with the corrected detector on the Fluoromax-4 spectrophotometer (see above). The presented BRET results are the average of the first five spectra collected over 1.5 min after addition of LH_2. Peak area was calculated by spectral deconvolution of each spectrum using the data analysis package in Igor Pro (Wavemetrics Inc.). Fluorescence quantum yields and anisotropy measurements were collected

on a Horiba Fluoromax4 spectrofluorometer equipped with automatic excitation and emission polarizers. QY measurements were performed on solutions well below 0.1 optical densities at points of excitation (400 nm), whereas best anisotropy results were obtained for concentrations approaching this limit. Quantum rod and Ppy concentrations were obtained using optical absorption measurements *via* a Varian Cary Bio100 UV-visible spectrophotometer (UV-vis). The transmission electron microscopy (TEM) results were obtained using a JEOL 2000EX transmission electron microscope operated at 100 kV. Samples were drop cast onto a carbon coated copper grids. The Fourier Transform Infrared (FTIR) data was acquired using a Nicolet 6700 FTIR spectrometer equipped with a diamond smart iTR attenuated internal reflectance accessory, and a liquid N_2 cooled MCT-A detector. Samples were drop cast as neat solutions, or dried powders on the ATR crystals. The TCSPC (PL decay) measurements were performed at Brookhaven National Laboratory (BNL) in the Center for Functional Nanomaterials (CFN) USER facility. PL decays were measured by TCSPC using a 420 nm pulsed laser excitation. The setup is based on a frequency doubled diode-pumped Ti:sapphire laser system (Newport Spectra Physics, 8 MHz repetition rate, 60 fs pulse width) and a Fluorotime 200 time-resolved fluorescence spectrometer (Picoquant GmbH). Fluorescence decays were collected at magic angle, detected by a microchannel plate photomultiplier (Hamamatsu, 25 ps response) and registered by a TCSPC module (Picoharp 300, Picoquant GmbH). Decay histograms were collected with a time resolution of 4 ps per channel and analyzed by biexponential decay model after correction for instrument response function.

Supporting Tables

Table S1: Optical and FRET parameters for QR BRET nanosystems.

			BRET Nanosystems					
QR(650)	**QR Absorption[1]**		**PPY-GRTS [2]**		**PPY-RE9 [3]**		**GRTS + $BtLH_2$ [4]**	
l/w	**λ_A (nm)**	**ε ($M^{-1}cm$)**	***J*** **(cm^6)**	***R_0*** **(nm)**	***J*** **(cm^6)**	***R_0*** **(nm)**	***J*** **(cm^6)**	***R_0*** **(nm)**
Small	623	6.11×10^5	7.33×10^{-12}	8.8	7.05×10^{-12}	7.3	7.63×10^{-12}	7.2
Medium	625	6.50×10^5	7.74×10^{-12}	8.8	7.54×10^{-12}	7.4	8.03×10^{-12}	7.2
Large	632	7.94×10^5	1.17×10^{-11}	9.4	1.05×10^{-11}	7.8	1.25×10^{-11}	7.8

[1)] The QR first absorption maxima (λ_A), and calculated extinction coefficient (ε). [2)] Calculated using PpyGRTS QY of 32% and emission maxima of 547 nm. 3) Calculated using a PpyRE9 QY of 12% and emission maxima of 617 nm. [4)] Calculated using estimated $BtLH_2$ QY of 10%, and emission maxima of 520 nm.

Table S2: Measured BRET ratios (*BR*), and normalized BRET ratios (*BR/QY*)

		BRET Ratios at *L* = 1					
QR(650)		**PPY-GRTS**		**PPY-RE9**		**GRTS + $BtLH_2$**	
l/w	**QY (%)**	***BR***	***BR/QY***	***BR***	***BR/QY***	***BR***	***BR/QY***
Small	4.1	6.9	1.7	9.1	2.3	12.0	3.0
Medium	10.7	17.2	1.6	12.1	1.1	11.0	1.0
Large	23.2	30.1	1.3	24	1.0	11.5	0.5

Table S3: Optical and FRET parameters for QR BRET nanosystems.

				BRET Nanosystems			
QR(615)		**QR Absorption[1]**		**PPY-GRTS [2]**		**BRET Ratios at *L* = 1**	
l/w	***QY(%)***	**λ_A (nm)**	**ε ($M^{-1}cm$)**	***J*** **(cm^6)**	***R_0*** **(nm)**	***BR***	***BR/QY***
Small	10.6	583	2.19×10^5	1.97×10^{-12}	7.0	8.5	0.8
Medium	30.0	597	3.07×10^5	3.14×10^{-12}	7.5	12.0	0.4
Large	51.2	602	3.48×10^5	3.76×10^{-12}	7.8	20.5	0.4

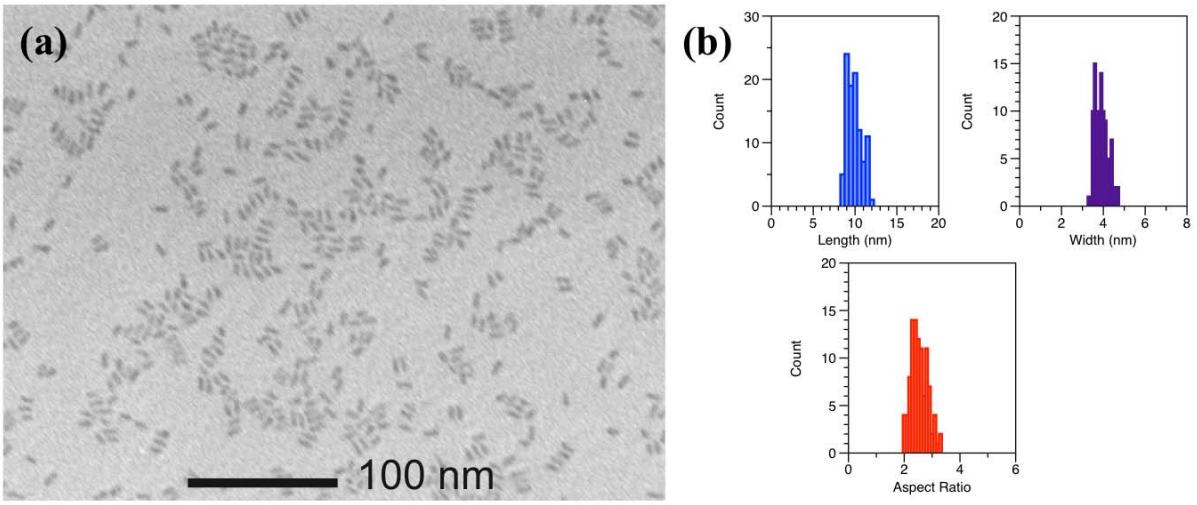

Figure S1. TEM micrograph (a) and statistical analysis (b) of CdSe-QR used to make QR(615) (l/w = 2.5 ± 0.3, l = 9.9 ± 0.9 nm, w = 3.9 ± 0.3 nm).

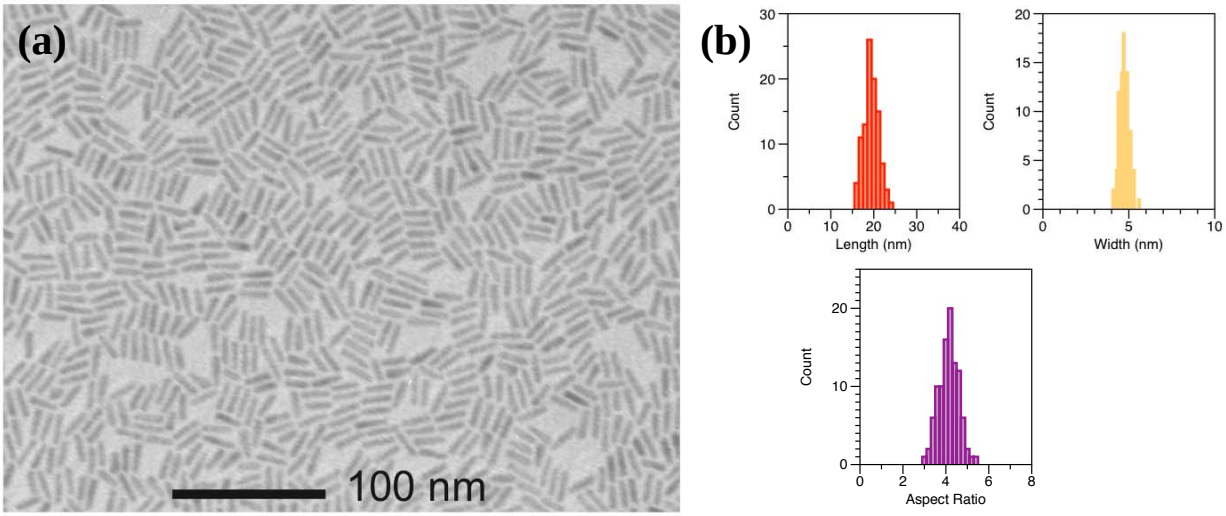

Figure S2. TEM micrograph (a) and statistical analysis (b) of CdSe-QR used to make QR(650) (l/w = 4.1 ± 0.4, l = 19.4 ± 1.6 nm, w = 4.7 ± 0.3 nm).

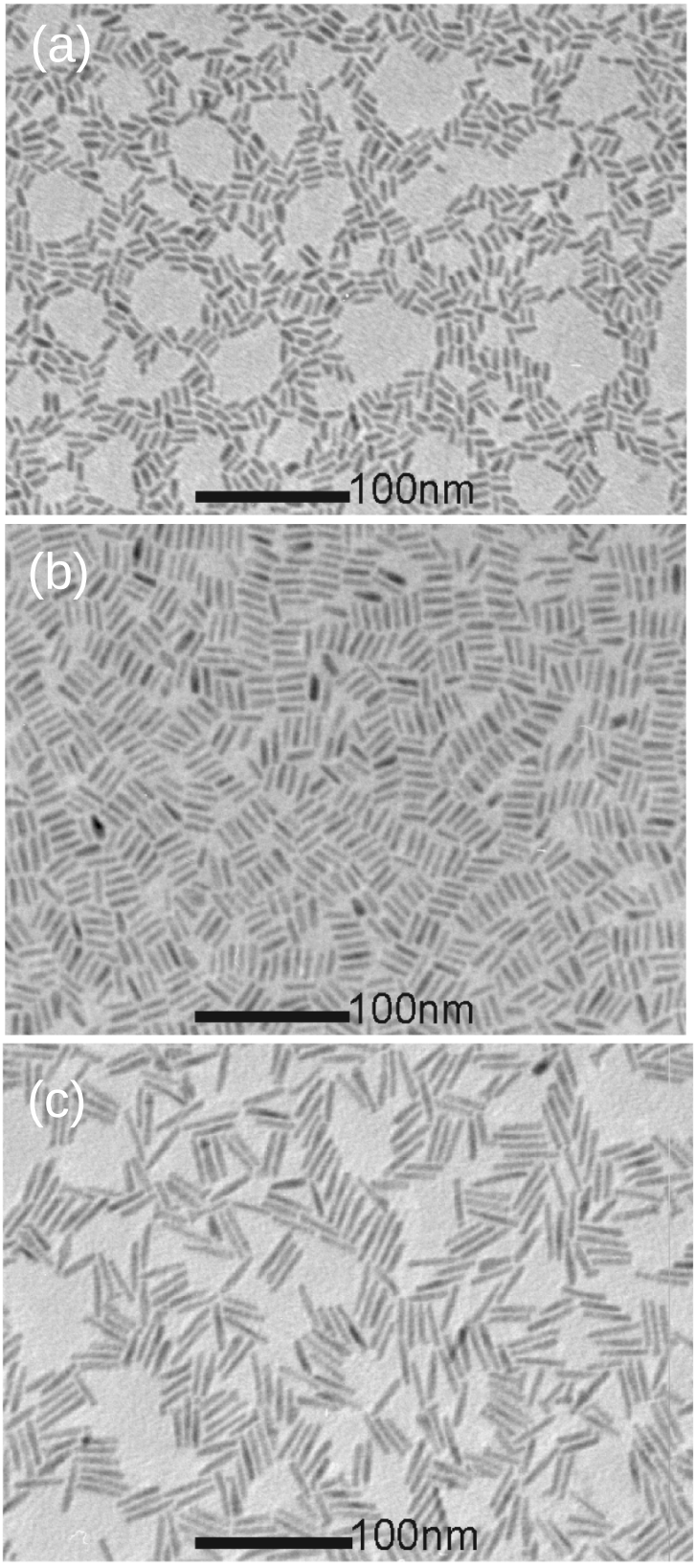

Figure S3: Additional TEM micrographs of QR(615)-*s* (a, l = 13.4 ±1.4 nm, w = 4.4 ± 0.3 nm), -*m* (b, l = 20.4 ± 1.4 nm, w = 4.6 ± 0.4 nm), and –*l* (c, l = 32.3 ±2.9 nm, w = 4.7 ± 0.3 nm).

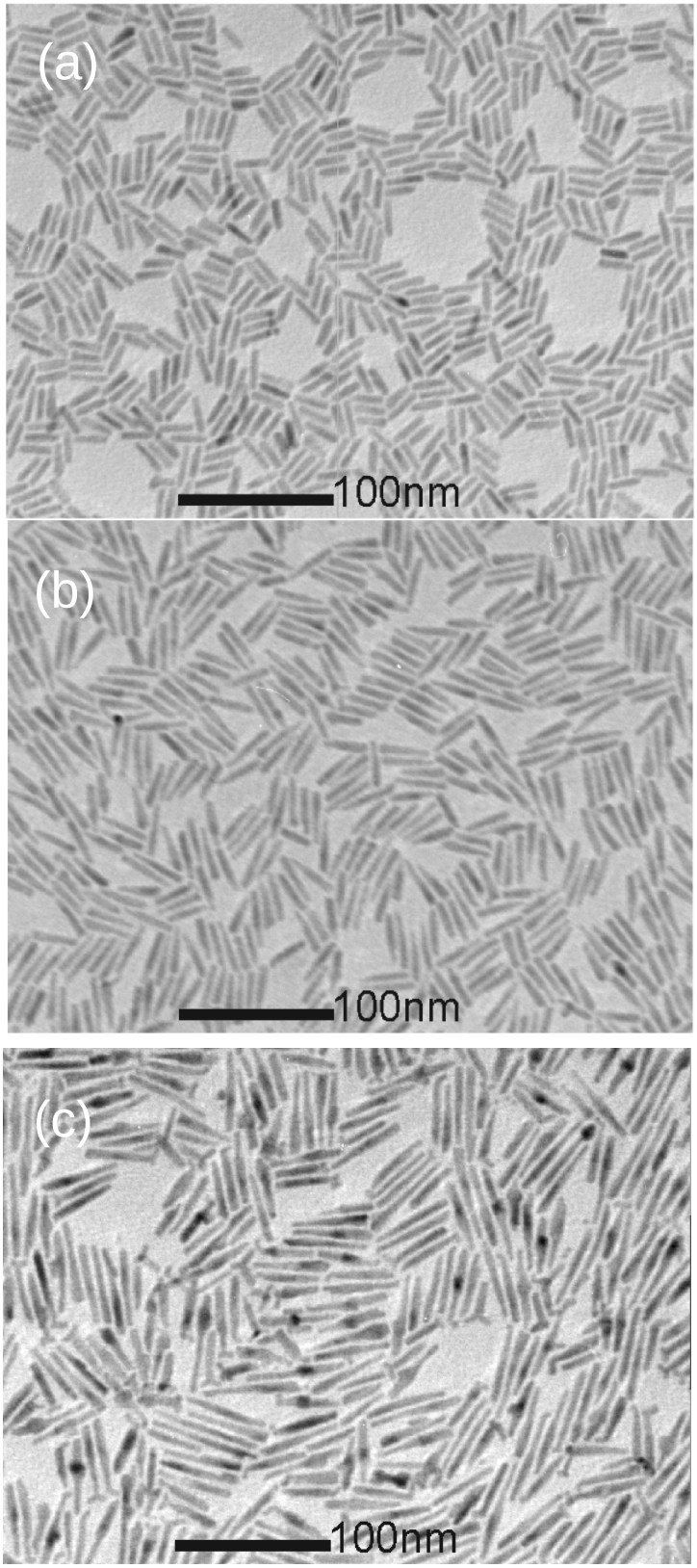

Figure S4: Additional TEM micrographs of QR(650)-*s* (a, *l* = 22.4 ±1.9 nm, *w* = 5.4 ± 0.4 nm), -*m* (b, *l* = 31.0 ±2.5 nm, *w* = 5.4 ± 0.3 nm), and –*l* (c, *l* = 50.1 ±6.1 nm, *w* = 5.7 ± 0.4 nm).

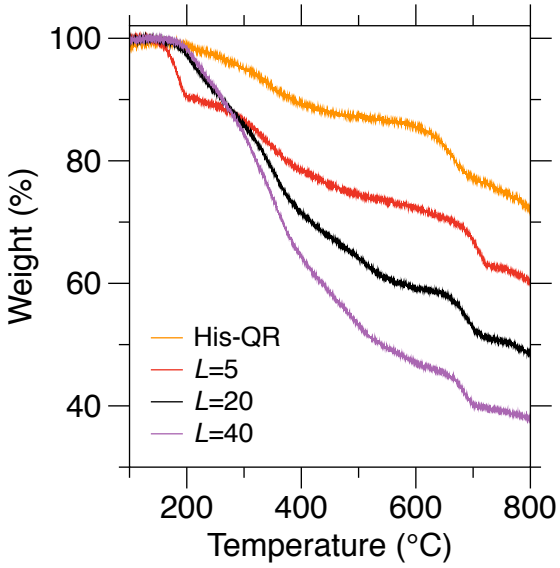

Figure S5: TGA results characterizing histidine-capped QRs (His-QR) before and after incubation with PpyGRTS at L = 5-40. The increasing mass loss is indicative of higher Ppy loading.

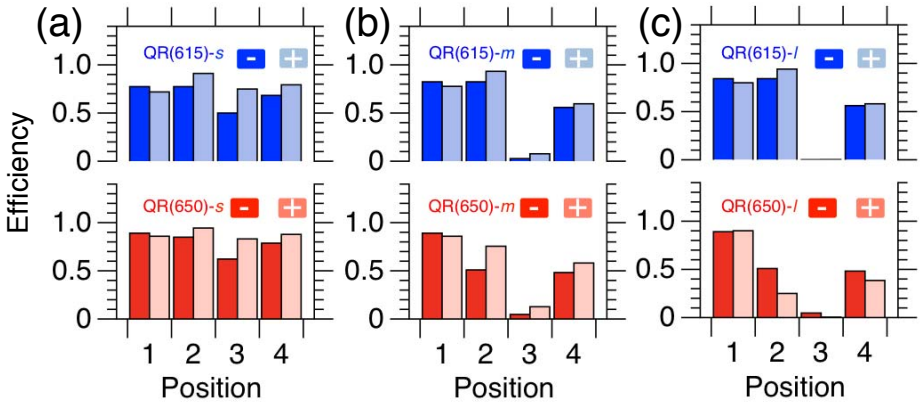

Figure S6: Calculated BRET efficiency for QR(615) and QR(650) –*s* (a), –*m* (b), and –*l* (c) with (+) and without (-) polarization considerations. Calculations are based on calculated dipole moments at position 1-4 of given QR after considerations of rod dimensions. See Figure 3d in main text for positions.

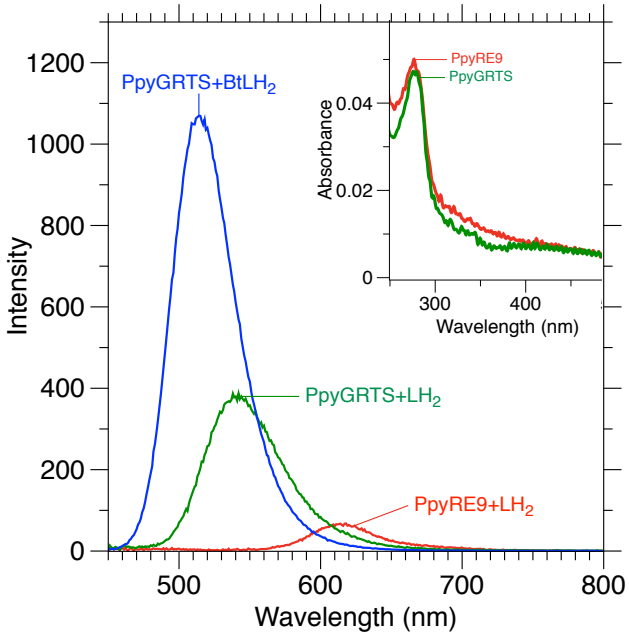

Figure S7: Bioluminescence spectra comparing the brightness of enzyme+substrate combinations under identical enzyme concentrations (insert) and experimental conditions. Results indicate Ppy+$BtLH_2$ has ~ 2.8x brightness of PpyGRTS+LH_2 and ~ 15.8x brightness of PpyRE9+LH_2.

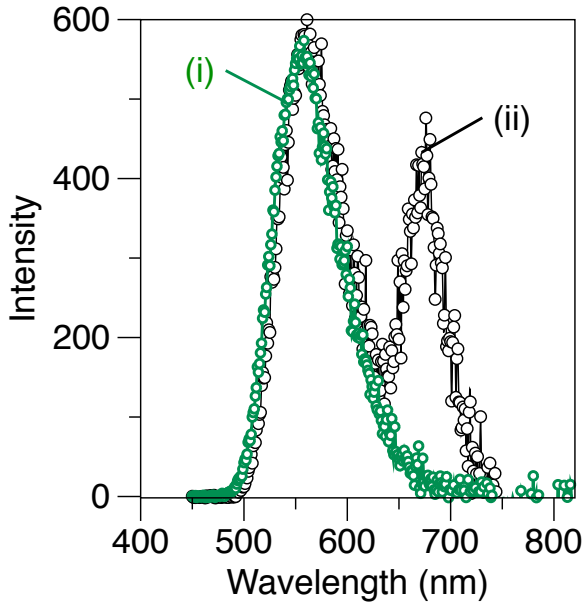

Figure S8: Bioluminescence spectra of PpyGRTS+LH_2 (i) and PpyGRTS+LH_2+PEG-QR(680) at L = 5 (ii). When using a PEG modified QR(680), the bioluminescence maxima of PpyGRTS+LH_2 is similar to the enzyme alone, an the QR(680) emission is lower than in a

typical BRET experiment, confirming that non-radiative transfer is possible when both components are in solution but not linked. Note the QR(680) is a different QR than used in the main text.

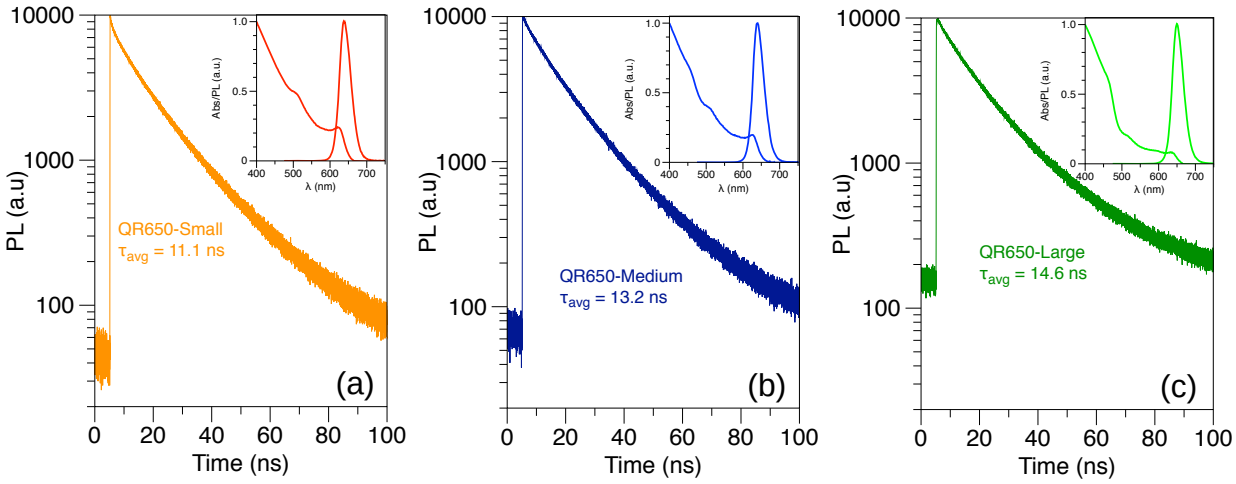

Figure S9: TCSPC PL-decay results for QR(650)-*s* (a), -*m* (b), and –*l* (c) before phase transfer. Biexponential fits were used to fit to the PL-decays, which were intensity weighted to average lifetimes (τ_{ave}) of τ_{ave} = 11.1 (a), 13.2 (b), and 14.6 ns (c) respectively.

Supporting References:

(1) Talapin, D. V.; Nelson, J. H.; Shevchenko, E. V.; Aloni, S.; Sadtler, B.; Alivisatos, A. P. Seeded Growth of Highly Luminescent CdSe/CdS Nanoheterostructures with Rod and Tetrapod Morphologies. *Nano Lett.* **2007**, *7*, 2951–2959.

(2) Alam, R.; Fontaine, D. M.; Branchini, B. R.; Maye, M. M. Designing Quantum Rods for Optimized Energy Transfer with Firefly Luciferase Enzymes. *Nano Lett.* **2012**, *12*, 3251–3256.

(3) Menagen, G.; Macdonald, J. E.; Shemesh, Y.; Popov, I.; Banin, U. Au Growth on Semiconductor Nanorods: Photoinduced *versus* Thermal Growth Mechanisms. *J. Am. Chem. Soc.* **2009**, *131*, 17406–17411.

(4) Branchini, B. R.; Ablamsky, D. M.; Murtiashaw, M. H.; Uzasci, L.; Fraga, H.; Southworth, T. L. Thermostable Red and Green Light-Producing Firefly Luciferase Mutants for Bioluminescent Reporter Applications. *Anal. Biochem.* **2007**, *361*, 253–262.

(5) Branchini, B. R.; Ablamsky, D. M.; Rosenberg, J. C. Chemically Modified Firefly Luciferase Is an Efficient Source of Near-Infrared Light. *Bioconjug. Chem.* **2010**, *21*, 2023–2030.

(6) Branchini, B. R.; Ablamsky, D. M.; Davis, A. L.; Southworth, T. L.; Butler, B.; Fan, F.; Jathoul, A. P.; Pule, M. A. Red-Emitting Luciferases for Bioluminescence Reporter and Imaging Applications. *Anal. Biochem.* **2010**, *396*, 290–297.

(7) Zylstra, J.; Amey, J.; Miska, N. J.; Pang, L.; Hine, C. R.; Langer, J.; Doyle, R. P.; Maye, M. M. A Modular Phase Transfer and Ligand Exchange Protocol for Quantum Dots. *Langmuir* **2011**, *27*, 4371–4379.

(8) Han, H.; Zylstra, J.; Maye, M. M. Direct Attachment of Oligonucleotides to Quantum Dot Interfaces. *Chem. Mater.* **2011**, *23*, 4975–4981.

(9) Doane, T. L.; Alam, R.; Maye, M. M. Functionalization of Quantum Tods with Oligonucleotides for Programmable Assembly with DNA Origami. *Nanoscale* **2015**, *7*, 2883–2888.

(10) Alam, R.; Zylstra, J.; Fontaine, D. M.; Branchini, B. R.; Maye, M. M. Novel Multistep BRET-FRET Energy Transfer Using Nanoconjugates of Firefly Proteins, Quantum Dots, and Red Fluorescent Proteins. *Nanoscale* **2013**, *5*, 5303.
(11) Alam, R.; Karam, L. M.; Doane, T. L.; Zylstra, J.; Fontaine, D. M.; Branchini, B. R.; Maye, M. M. Near Infrared Bioluminescence Resonance Energy Transfer from Firefly Luciferase—quantum Dot Bionanoconjugates. *Nanotechnology* **2014**, *25*, 495606.
(12) Shaviv, E.; Salant, A.; Banin, U. Size Dependence of Molar Absorption Coefficients of CdSe Semiconductor Quantum Rods. *ChemPhysChem* **2009**, *10*, 1028–1031.
(13) Lakowicz, J. R. *Principles of Fluorescence Spectroscopy*; 3rd ed.; Springer: New York, 2006.
(14) Clapp, A. R.; Medintz, I. L.; Mattoussi, H. Förster Resonance Energy Transfer Investigations Using Quantum-Dot Fluorophores. *ChemPhysChem* **2006**, *7*, 47–57.